Catalytic Dehydrogenative Coupling of Stannanes by Alkoxysilyl Heterobimetallic Complexes: Influence of the Assembling Ligand†

Pierre Braunstein,*,‡ Jérôme Durand,‡ Xavier Morise,‡ Antonio Tiripicchio,§ and Franco Ugozzoli§

Laboratoire de Chimie de Coordination, UMR CNRS 7513, Université Louis Pasteur, 4, rue Blaise Pascal, F-67070 Strasbourg Cédex, France, and Dipartimento di Chimica Generale ed Inorganica, Chimica Analitica, Chimica Fisica, Università di Parma, Centro di Studio per la Strutturistica Diffrattometrica del CNR, Parco Area delle Scienze 17A, I-43100 Parma, Italy

Received August 16, 1999

The heterobimetallic complexes $[(OC)_3(R'_3Si)\overline{Fe(\mu\text{-P-Z})Pd}(\eta^3\text{-allyl})]$ (**1**, P-Z = $Ph_2PNHPPh_2$ (dppa); **2**, P-Z = $Ph_2P(o\text{-}C_5H_4N)$ (Ph_2Ppy); **3**, P-Z = $Ph_2PCH_2PPh_2$ (dppm); R'_3 = $(OMe)_3$, $Me(OSiMe_3)_2$) are very efficient catalysts for the dehydrogenative coupling of tin hydrides R_3SnH (R = Ph, ^{n}Bu). Besides establishing that siloxy complexes are more active catalysts than their alkoxysilyl counterparts, the present study shows that modifications in the nature of the assembling functional phosphine ligand P-Z result in variations of catalyst efficiency, expressed by the TON (overall turnover number) and TOF (maximum turnover frequency) values and lifetime. The Ph_2Ppy-bridged complexes are the most efficient catalysts, and in the case of $^n Bu_3SnH$, TON and TOF values higher than 1.2×10^6 and 2×10^8, respectively, have been observed. A marked difference in reactivity is also observed between the diphosphine ligands dppa and dppm, with the dppa-bridged complexes being more active than their dppm analogues. The new complex $[(OC)_3\{(Me_3SiO)_2MeSi\}\overline{Fe(\mu\text{-}Ph_2Ppy)Pd}(\eta^3\text{-allyl})]$ (**2b**) prepared in the course of this work has been structurally characterized by X-ray diffraction.

Introduction

The development of the chemistry of compounds containing a tin−tin bond mainly results from the numerous industrial,[1−4] biological,[2−7] and synthetic applications of distannanes. In the last case they are usually employed as radical sources,[8−13] as precursors to tin−metal complexes[14,15] or in palladium-catalyzed cross-coupling reactions for fine chemical synthesis.[16−19] Although numerous procedures are known to allow tin−tin bond formation,[2,3,20] new syntheses of distannanes are still being sought. The dehydrogenative coupling of tin hydrides appears as an efficient method. It is known to be facilitated by reagents such as amines[19] and amides.[21] Surprisingly, examples of this reaction being catalyzed by transition-metal complexes remain scarce.[22−27] This approach is, however, of current interest owing to recent advances in the synthesis of high-

* To whom correspondence should be addressed. E-mail: braunst@chimie.u-strasbg.fr.

† Dedicated to our friend and colleague Professor H. Vahrenkamp, on the occasion of his 60th birthday, with our warmest congratulations and good wishes.

‡ Université Louis Pasteur.
§ Università di Parma.

(1) Evans, C. J. In *Chemistry of Tin*; Harrison, P. G., Ed.; Blackie: Glasgow, Scotland, 1989; pp 421−453, and references therein.
(2) Davies, A. G.; Smith, P. G. In *Comprehensive Organometallic Chemistry*; Abel, E. W., Stone, F. G. A., Wilkinson, G., Eds.; Pergamon: Oxford, U.K., 1982; Vol. 2, pp 519, and references therein.
(3) Wardell, J. L. In *Encyclopedia of Inorganic Chemistry*; King, R. B., Ed.; Wiley: New York, 1994; Vol. 8, pp 4172, and references therein.
(4) Weis, R. W. *Organometallic Compounds*, 2nd ed.; Springer: New York, 1973; Vol. II, first supplement, pp 826−832, and references therein.
(5) Davies, A. G.; Smith, P. G. *Adv. Inorg. Chem. Radiochem.* **1980**, *23*, 1 and references therein.
(6) Cusack, P.; Smith, P. G. *Rev. Silicon, Germanium, Tin Lead Compd.* **1983**, *7*, 1.
(7) Selwyn, M. J. In *Chemistry of Tin*; Harrison, P. G., Ed.; Blackie: Glasgow, Scotland, 1989; pp 359−396, and references therein.
(8) Pereyre, M.; Pommier, J. C. *J. Organomet. Chem.* **1976**, *1*, 161.
(9) Keck, G. E.; Byers, J. H. *J. Org. Chem.* **1985**, *50*, 5442.
(10) Storck, G.; Sher, P. *J. Am. Chem. Soc.* **1983**, *105*, 6765.
(11) Baldwin, J. E.; Kelly, D. R.; Ziegler, C. B. *J. Chem. Soc., Chem. Commun.* **1984**, 133.
(12) Keck, G. E.; Tafesh, A. M. *J. Org. Chem.* **1989**, *54*, 5845.
(13) Snider, B. B.; Buckman, B. O. *J. Org. Chem.* **1992**, *57*, 4883.
(14) (a) Quintard, J. P.; Pereyre, M. *Rev. Silicon, Germanium, Tin Lead Compd.* **1980**, *4*, 154. (b) Abel, E. W.; Moorhouse, S. *J. Organomet. Chem.* **1970**, *24*, 687.
(15) Holt, M. S.; Wilson, W. L.; Nelson, J. H. *Chem. Rev.* **1989**, *89*, 11.
(16) Diederich, F.; Stang, P. J. *Metal-Catalyzed Cross-Coupling Reactions*; Wiley-VCH: Weinheim, Germany, 1998.
(17) Farina, V.; Krishnamurthy, V.; Scott, W. J. *Organic Reactions*; Wiley: New York, 1997; Vol. 50, pp 1−652, and references therein.
(18) Stille, J. K. *Angew. Chem., Int. Ed. Engl.* **1986**, *25*, 508 and references therein.
(19) Davies, A. G.; Osei-Kissi, D. K. *J. Organomet. Chem.* **1994**, *474*, C8.
(20) Sita, L. R. *Adv. Organomet. Chem.* **1995**, *38*, 189 and references therein.
(21) Puff, H.; Breuer, B.; Gehrke-Brinkmann, G.; Kind, P.; Reuter, H.; Schub, W.; Wald, W.; Weideinbrück, G. *J. Organomet. Chem.* **1989**, *363*, 265.
(22) Bugamin, N. A.; Gulevich, Y. V.; Beletskaya, I. P. *Izv. Akad. Nauk SSSR, Ser. Khim.* **1982**, 2639.
(23) Mitchell, T. N.; Amamria, A.; Killing, H.; Rutschow, D. *J. Organomet. Chem.* **1986**, *304*, 257.
(24) Zhang, H. X.; Guibé, F.; Balavoine, G. *J. Org. Chem.* **1990**, *55*, 1859.
(25) Voskoboynikov, A. Z.; Beletskaya, I. P. *New J. Chem.* **1995**, *19*, 723.

10.1021/om9906619 CCC: $19.00
Publication on Web 01/22/2000

molecular-weight polystannanes, a promising class of new polymers, by dehydropolymerization of tin dihydrides.[27−30]

We have recently reported that trialkoxysilyl and siloxy heterobimetallic Fe−Pd complexes of the types **A** and **B** were efficient catalysts for the dehydrogenative coupling of stannanes.[26,27] Interestingly, this reaction

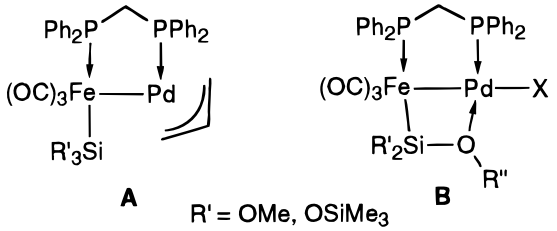

A **B**

R' = OMe, OSiMe$_3$
R" = Me, SiMe$_3$
X = Cl, SnPh$_3$

enabled us to evaluate the role of the heterobimetallic structure of the catalysts and the influence of the ligand environment on the active metal center.[27]

Although elementary transformations appear to take place at palladium, the silyl ligand bound to the iron center plays a key role in the catalytic process.[27] This ligand is involved in the stabilization of reactive intermediates via formation of O→Pd interactions, whereas owing to its hemilabile behavior a vacant coordination site at the Pd center may be released for an incoming substrate molecule (equilibrium **B** ⇌ **C**, Scheme 1). We have observed that substituent modifications at silicon resulted in considerable variations of catalyst performances and lifetime. We have also established that the heterobimetallic Fe−Pd silyl derivatives were more efficient catalysts than mononuclear Pd complexes and retained their bimetallic structure throughout the process.[27]

Scheme 1

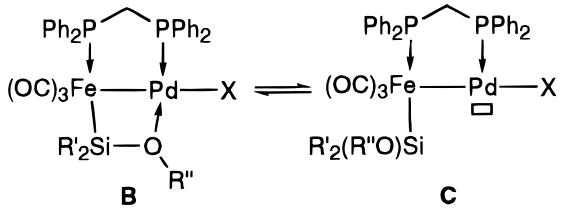

B **C**

Herein, we report our investigations aimed at evaluating the influence of the nature of the assembling ligand on the dehydrogenative coupling of Ph_3SnH and $^nBu_3SnH$ catalyzed by Fe−Pd−allyl heterobimetallic complexes. For this purpose, the catalytic activity of dppa ($Ph_2PNHPPh_2$), dppm ($Ph_2PCH_2PPh_2$), and Ph_2-Ppy ($Ph_2P\{o\text{-}C_5H_4N\}$) bridged derivatives has been determined. Important variations in catalyst efficiency and lifetime have been observed.

Results

1. Catalysts. The Fe−Pd heterobimetallic complexes pictured in Chart 1 have been used in the present study as catalysts for the dehydrogenative coupling of Ph_3-SnH and $^nBu_3SnH$.

Chart 1

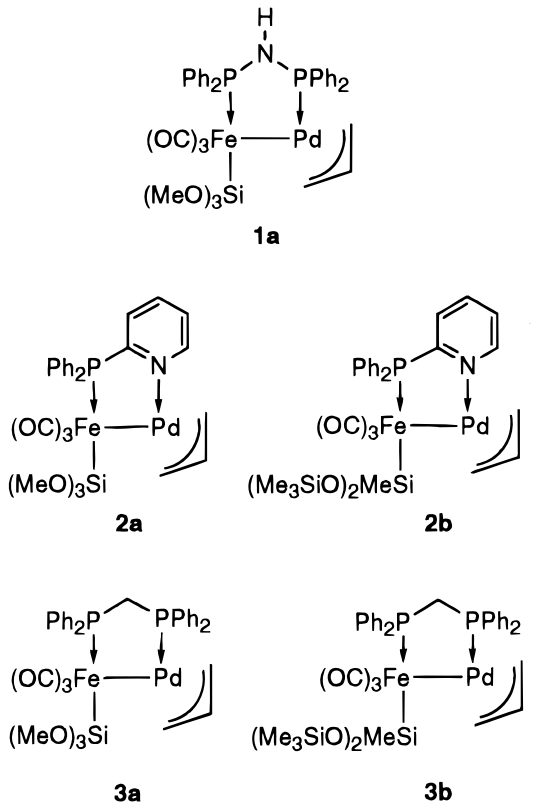

1a **2a** **2b** **3a** **3b**

We have previously reported the synthesis of **1a**,[31] **2a**,[32] and **3a**,**b**.[32,33] The new complex [(OC)$_3${(Me$_3$-SiO)$_2$MeSi}Fe(μ-Ph$_2$Ppy)Pd(η^3-allyl)] **(2b)** was obtained as an air-stable yellow-orange powder in 64% yield (based on Pd) by reaction of the dinuclear complex [Pd-(η^3-C_3H_5)(μ-Cl)]$_2$ with 2 molar equiv of the iron metalate K[Fe{SiMe(OSiMe$_3$)$_2$}(CO)$_3$(Ph$_2$Ppy-*P*)] (**5**)[34] (obtained by deprotonation of the hydrido complex **4**; Scheme 2). Its IR spectrum (KBr) shows three ν(CO) vibrations, at 1955 m, 1895 s, and 1873 vs cm^{-1}, indicative of the *mer* arrangement of the three carbonyl ligands around the Fe center. The $^{31}P\{^1H\}$ NMR spectrum contains a singlet at δ 73.3 ppm. Other spectroscopic data are given in the Experimental Section. The structure of **2b** was confirmed by an X-ray diffraction study (Figure 1). Selected bond distances and angles are given in Table 1.

The coordination geometry around the Fe atom is distorted octahedral; that of the Pd atom involves the Fe atom, the N atom from the Ph_2Ppy ligand, and the C(9), C(10), and C(11) carbon atoms from the allylic group interacting in a η^3 fashion. When the allylic group is considered as occupying two coordination sites, the environment around the Pd atom is distorted square planar. Whereas the N−Pd−Fe angle (92.8(4)°) is regular, the P−Fe−Pd angle of 75.6(2)° is very acute,

(26) Braunstein, P.; Morise, X.; Blin, J. *J. Chem. Soc., Chem. Commun.* **1995**, *14*, 1455.
(27) Braunstein, P.; Morise, X. *Organometallics* **1998**, *17*, 540.
(28) Imori, T.; Lu, V.; Cai, H.; Tilley, T. D. *J. Am. Chem. Soc.* **1995**, *117*, 9931.
(29) Babcock, J. R.; Sita, L. R. *J. Am. Chem. Soc.* **1996**, *118*, 12481.
(30) Lu, V.; Tilley, T. D. *Macromolecules* **1996**, *29*, 5763.
(31) Braunstein, P.; Durand, J.; Kickelbick, G.; Knorr, M.; Morise, X.; Pugin, R.; Tiripicchio, A.; Ugozzoli, F. *J. Chem. Soc., Dalton Trans.* **1999**, 4175.
(32) Braunstein, P.; Faure, T.; Knorr, M.; Balegroune, F.; Grandjean, D. *J. Organomet. Chem.* **1993**, *462*, 271.
(33) Braunstein, P.; Knorr, M.; Piana, H.; Schubert, U. *Organometallics* **1991**, *10*, 828.
(34) Knorr, M.; Braunstein, P. *Bull. Soc. Chim. Fr.* **1992**, *129*, 663.

Scheme 2

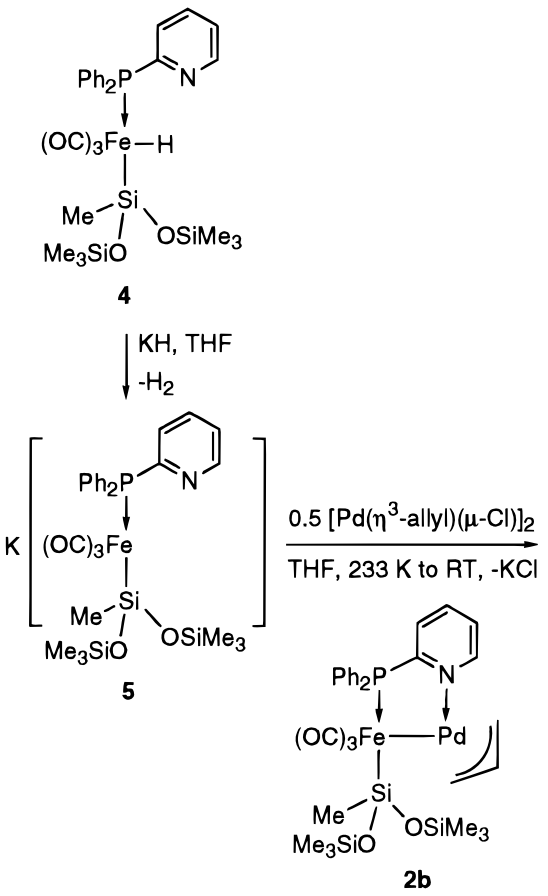

probably because of the narrow P−C(4)−N angle (109.7-(13)°) and the rather long Fe−Pd bond (2.678(4) Å). The value of the Fe−Pd bond length falls in the range (2.544-(4)−2.850(2) Å) of those reported for similar structures containing a P,P (dppm or dppa) bridging ligand.[31−33,35,36]

2. Dehydrogenative Coupling of R_3SnH. *The data reported below refer to average values determined for a minimum of three catalytic runs. Note that in the presence of a large excess of radical scavenger (TEMPO, galvinoxyl) no significant variations of the catalysis results were observed.*

(i) Ph_3SnH. The catalytic activity may be monitored by either the formation of Ph_6Sn_2 (**3a**) or the volume of H_2 released (**2a**,**b**) (eq 1),[26,27] as described in the Experimental Section. Note that, under the reaction

$$2\ R_3SnH \xrightarrow[CH_2Cl_2]{cat.} R_6Sn_2 + H_2 \quad (R = Ph, Bu) \qquad (1)$$

conditions used, the decrease in reaction rate and eventually the end of the reaction are due to the fading of the catalyst activity and not to a decrease in substrate concentration.[26]

Figure 2 shows the plot of TON vs time for the trimethoxysilyl complexes **1a**, **2a**, and **3a**, and selected data are given in Table 2. For the diphosphine-containing catalysts **1a** and **3a** long reaction times, or catalyst

(35) Braunstein, P.; Knorr, M.; Schubert, U.; Lanfranchi, M.; Tiripicchio, A. *J. Chem. Soc., Dalton Trans.* **1991**, 1507.
(36) Braunstein, P.; Knorr, M.; Tiripicchio, A.; Tiripicchio-Camellini, M. *Angew. Chem., Int. Ed. Engl.* **1989**, *28*, 1361.

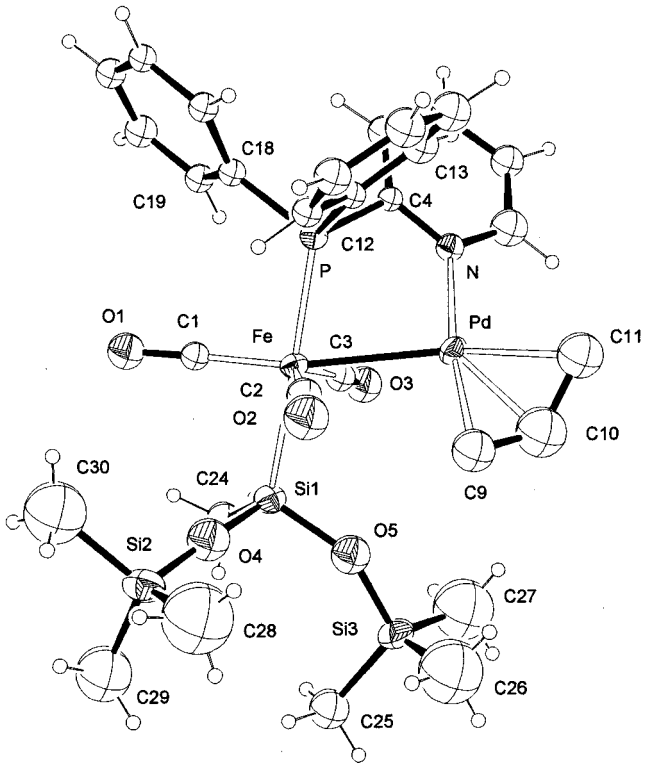

Figure 1. View of the molecular structure of complex **2b**.

Table 1. Selected Bond Lengths (Å) and Angles (deg) for 2b

Pd−Fe	2.678(4)	Pd−N	2.114(16)
Pd−C9	2.20(3)	Pd−C10	2.12(4)
Pd−C11	2.18(3)	C10−C11	1.44(4)
Fe−P	2.210(6)	Fe−Si1	2.331(6)
Fe−C1	1.71(2)	Fe−C2	1.75(2)
Fe−C3	1.77(2)	Si1−O4	1.65(2)
Si1−O5	1.66(2)	Si1−C24	1.84(2)
Si2−O4	1.55(2)	Si3−O5	1.58(2)
N−C4	1.32(2)	N−C8	1.34(3)
O1−C1	1.20(2)	O2−C2	1.17(3)
O3−C3	1.18(2)	C9−C10	1.35(4)

Fe−Pd−N	92.8(4)	Pd−Fe−P	75.6(2)
C2−Fe−Pd	82.7(7)	C3−Fe−Pd	67.4(6)
C2−Fe−C3	140.7(10)	C1−Fe−C3	108.0(9)
C1−Fe−C2	105.9(10)	Si1−Fe−C3	81.6(7)
Si1−Fe−C2	82.8(7)	Si1−Fe−C1	84.1(6)
P−Fe−C3	98.0(7)	P−Fe−C2	98.7(8)
P−Fe−C1	94.2(6)	P−Fe−Si1	178.0(2)
Si1−O4−Si2	172.5(13)	Si1−O5−Si3	152.0(10)
Fe−C1−O1	178.0(17)	Fe−C2−O2	176.1(22)
Fe−C3−O3	174.2(18)	P−C4−N	109.7(13)
C9−C10−C11	129(3)		

lifetimes, are observed, as evidenced by the plateau being reached after ca. 48 h. The overall catalytic activity of the dppa complex **1a** (TON = 1550) is, however, more than twice that of its dppm analogue **3a** (TON = 700). This may be related to the higher maximum reaction rate (TOF; see Table 2) observed for **1a**. The situation for the Ph_2Ppy-bridged complex **2a** is, however, somewhat different. The reaction is much faster (the plateau is reached after only ca. 30 min) and the TOF value is considerably higher (ca. 1.70×10^5, Table 2). However, this rate is only maintained for a few seconds after an induction period of ca. 5 s, resulting in the total catalytic activity being in the same range as that of **1a** (TON = 1460; Table 2). For comparison, we found it of interest to determine the catalytic activity

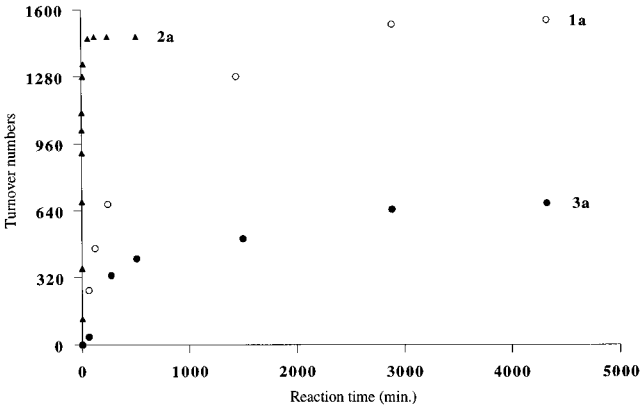

Figure 2. Catalytic dehydrogenative coupling of Ph_3SnH: plot of TON vs time for the complexes **1a**, **2a**, and **3a**.

Table 2. Selected Catalysis Data for the Dehydrogenative Coupling of Ph_3SnH Catalyzed by 1a, 2a,b, or 3a,b

catalyst	TON max[a]	plateau, h[b]	TOF[c]
1a	1550	48	ca. 260
2a	1460	0.5	ca. 1.70×10^5
3a[27]	700	48	ca. 100
2b	1850	0.25	ca. 2.10×10^5
3b[27]	1630	1	ca. 1.98×10^5

[a] Total catalytic activity expressed in turnover numbers (average value of a minimum of three experiments). [b] Time after which the plateau is reached. [c] Maximum turnover frequency expressed in TON h^{-1}.

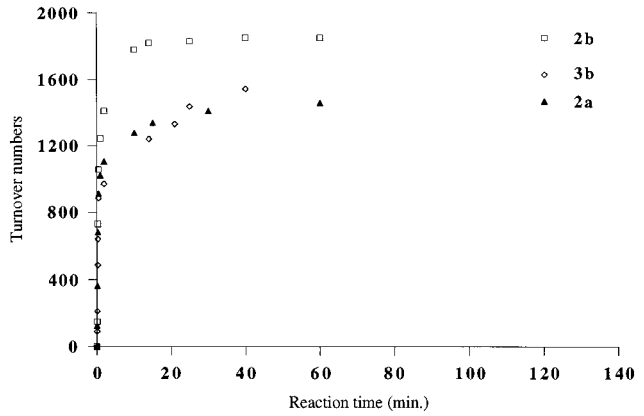

Figure 3. Catalytic dehydrogenative coupling of Ph_3SnH: comparative plot of TON vs time for the pairs of complexes **2a** and **2b** (same assembling ligand) and **2b** and **3b** (same siloxy ligand).

of the Ph_2Ppy-bridged siloxy complex **2b**. It is a more efficient catalyst than its trimethoxysilyl counterpart **2a** (higher TON and TOF values; Table 2). However, it displays a shorter lifetime (plateau reached after ca. 15 min). Figure 3 illustrates the comparison between **2a** and **2b**, which have the same assembling ligand, and between **2b** and **3b**, which have the same siloxy ligand. The last complex has been investigated previously.[27]

(ii) ^{n}Bu$_3$SnH. The reactivity of the trimethoxysilyl complexes **1a** and **2a** has also been evaluated with regard to the dehydrogenative coupling of ^{n}Bu$_3$SnH. The volume of H_2 released was monitored and converted into turnover numbers. Selected catalysis data are given in Table 3 and compared with those previously reported for **3a**.[27] The plots of turnover numbers vs time obtained

Table 3. Selected Catalysis Data for the Dehydrogenative Coupling of Bu_3SnH Catalyzed by 1a, 2a, or 3a

catalyst	TON max[a]	plateau, min[b]	TOF[c]
1a	ca. 500 000	120	ca. 5×10^6
2a	>1 200 000	*d*	*d*
3a[27]	ca. 114 000	1	ca. 23×10^6

[a] Total catalytic activity expressed in turnover numbers (average value of a minimum of three experiments). [b] Time after which the plateau is reached. [c] Maximum turnover frequency expressed in TON h^{-1}. [d] Not determined.

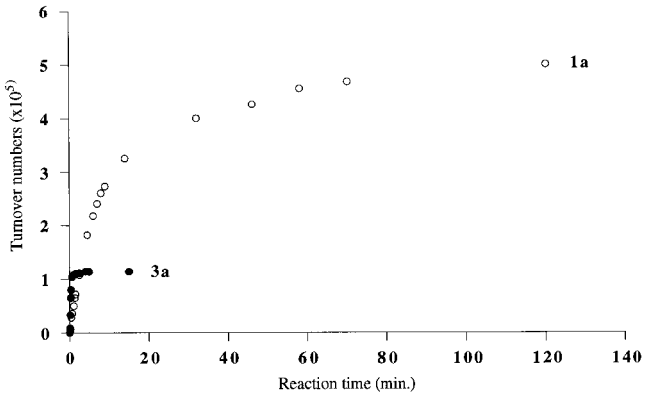

Figure 4. Catalytic dehydrogenative coupling of ^{n}Bu$_3$SnH: plot of TON vs time for the complexes **1a** and **3a**.

for **1a** and **3a** are shown in Figure 4, which illustrates the difference between the dppa and dppm complexes. Very high reaction rates and TON values, accompanied by a short catalyst lifetime (ca. 1 min), have been reported for the dppm complex **3a** (Table 3).[27] For the dppa complex **1a**, the reaction proceeds more slowly, the TOF value is ca. 5×10^6, and the plateau is only reached after 2 h (Figure 4, Table 3). This enhanced catalyst lifetime combined with a slow decrease of the reaction rate (after 8 min the turnover frequency is still $>1 \times 10^6$) account for **1a** being a much more efficient catalyst than **3a** (TON values of 500 000 and 114 000, respectively). In the case of the Ph_2Ppy complex **2a** no reliable catalysis data could be obtained, the reaction being extremely fast. We observed the consumption of more than 2.5×10^6 molar equiv of ^{n}Bu$_3$SnH within a few seconds.

Discussion

Mechanistic aspects of the dehydrogenative coupling of tin hydrides catalyzed by heterobimetallic Fe−Pd alkoxysilyl and siloxy complexes have been discussed in a previous paper.[27] Despite the very high reaction rates observed in the case of alkylstannanes, a σ-bond metathesis type mechanism or a succession of oxidative-addition and reductive-elimination steps were preferred to a radical chain mechanism. This is corroborated by the fact that radical scavengers, such as TEMPO or galvinoxyl, did not affect the catalysis measurements. Although it is always difficult to be sure of the true nature of a catalytic species, particularly in systems that display activities as high as those encountered in this work, we believe from in situ spectroscopic measurements on the less active systems (which allowed a higher catalyst concentration) that the bimetallic framework of the catalyst is retained throughout the reaction

and that elementary transformations take place at Pd. The role of the iron fragment is therefore to provide the Pd center with a suitable ligand environment through the metal−metal bonding, the assembling phosphine, and the silyl ligand. The last species is involved in the stabilization of reactive intermediates by its ability to develop bridging SiO→Pd interactions. As a result, substituent modifications at silicon should lead to important variations in catalyst performances and lifetime. In the present study, we have indeed found that siloxy complexes are much more active catalysts (precursors) in the dehydrogenative coupling of Ph_3SnH than their trialkoxysilyl counterparts: higher TONs and TOFs are obtained for **2b** and **3b** than for their trialkoxysilyl analogues **2a** and **3a**, respectively. This would be related to the oxygen donor capacity of siloxy ligands (Fe−Si−O−SiR_3) being lower than that of alkoxysilyl ligands (Fe−Si−O−CR_3), owing to the more electropositive character of the Si atom. Consequently, the SiO→Pd interactions are less stabilizing in the former case, providing a more accessible coordination site at Pd for an incoming substrate molecule (stannane). This results in higher reaction rates and TONs. However, a shorter catalyst lifetime is observed, owing to this lower stabilization (see, for example, catalysis data for **3a** and **3b**; Table 2).

We have verified the purity of the distannanes isolated after catalysis by ^{119}Sn NMR spectroscopy (see Experimental Section). Analysis of the reaction mixtures did not indicate the presence of products resulting from rearrangement of the substituents at tin. Only in the case of ^{n}Bu_3SnH were traces (<2%) of (^{n}$Bu_3Sn)_2O$ detected, which originate from adventitious oxidation.

The nature of the assembling phosphine in these bimetallic complexes plays a major role in providing additional stability.[35,36] It is certainly involved in the retention of the bimetallic structure of the catalysts during the reaction process, a factor which may largely contribute to the higher efficiency of Fe−Pd complexes in the catalytic dehydrogenative coupling of stannanes compared to Pd mononuclear complexes. Furthermore, the assembling ligand exerts a direct influence on the catalyst performances through its functional group coordinated to the active Pd center. This accounts for the important variations observed in the TON and TOF values as well as in catalyst lifetime for the dppa, Ph_2Ppy, and dppm complexes **1**−**3**, respectively. In the case of complexes **1a** and **3a**, replacement of the CH_2 group in **3a** by the amino function NH leads to improved catalyst efficiency. Indeed, the TON and TOF values obtained with **1a** for the dehydrogenative coupling of Ph_3SnH are more than twice those found for **3a**, whereas long lifetimes are noted for both catalysts (Table 2). The situation is slightly different with ^{n}Bu_3SnH. Surprisingly, the TOF observed for **1a**, although it is very high (ca. 5×10^6), is now lower than that obtained with **3a** (ca. 23×10^6). However, a much longer lifetime and only a slow decrease in the reaction rate (a turnover frequency $>1 \times 10^6$ is still observed after 8 min) compensate for this drawback and account for the former being a more efficient catalyst than the latter (Table 3).

As expected, more important effects on catalytic performances are observed when the nature of the donor group of the assembling ligand coordinated to the Pd center is changed. Thus, complexes **2**, in which a pyridine ligand is bound to Pd, are much more active than their dppa and dppm counterparts (Figures 2−4, Tables 2 and 3). Not only are higher TONs obtained, but improved TOFs are also observed. However, this higher reactivity is accompanied by a shorter lifetime of the catalysts. In the case of the dehydrogenative coupling of ^{n}Bu_3SnH, the reaction rate is too high to be determined. We estimate that it is $>2 \times 10^8$ TON h^{-1}.

Although various factors may be invoked, it seems reasonable to assume that the variations of reactivity of complexes **1**−**3** for the dehydrogenative coupling of tin hydrides result from the assembling ligands having different electronic and steric influences on the Pd center. Thus, the higher reactivity and shorter lifetime of **2**, in comparison to **1** and **3**, may probably be ascribed to the lower electron donating property[37] and/or the lower steric hindrance of the pyridine ligand vs the Ph_2P groups of dppm and dppa. When **2b** is compared with its dppm analogue,[32] the electronic effect of the pyridine compared to the Ph_2P group also manifests itself in the downfield shift of the ^{1}H NMR resonances of the protons H^1 and H^2 of the CH_2 group trans to the nitrogen (see Experimental Section). The relative effects of the diphosphine ligands in complexes **1** and **3** appear more subtle. One factor might be the lower electron-donating property of dppa compared to that of dppm. Indeed, the ν(CO) vibrations of the iron carbonyls are observed at higher wavenumbers for dppa-containing Fe mononuclear or Fe−Pd heterobimetallic complexes compared to their dppm analogues.[31] Structural aspects at Pd may also be considered. Indeed, we have observed slight differences in the bond distances and angles of [$(OC)_3$Fe-{μ-Si$(OMe)_2$(OMe}(μ-*P*,*P*)PdCl] (**6**, *P*,*P* = dppm;[36] **7**, *P*,*P* = dppa).[31] For example, Pd−O and Pd−Cl bond distances are longer in **7**, whereas the P−N−P angle in **7** (121.8(12)°) is more obtuse than the P−C−P angle in **6** (112.0(1)°). It is noteworthy that these complexes are stabilized by a SiO→Pd interaction and are thus analogous to intermediates formed during the catalytic process.[27]

Besides the fact that we have developed highly active catalysts for the formation of distannanes, the dehydrogenative coupling of tin hydrides represents a remarkable tool for studying the reactivity of heterobimetallic Fe−Pd silyl systems. Comparisons between catalysts have involved modification of one of the variables while maintaining the others constant. After having witnessed the effect of the metal−metal bonding and substituent modifications at Si on the catalytic activity and reaction kinetics, we have now observed that the catalyst performances are also dependent on the nature of the assembling difunctional ligand. We have thus established that Ph_2Ppy-bridged systems are more active than their dppa analogues, themselves being more active than dppm-bridged complexes. We have now the possibility of tuning the reactivity of the Pd center, in heterobimetallic Fe−Pd silyl complexes, by modifying the nature of the ligands carried by the Fe fragment. This work represents a further insight into

(37) Basolo, F.; Pearson, R. G. *Mechanisms of Inorganic Reactions*, 2nd ed.; Wiley: New York, 1967; pp 351−453.

homogeneous bimetallic catalysis and contributes to a better understanding of the influence of a metal center (Fe) on the reactivity of the adjacent metal (Pd).[38]

Experimental Section

All the reactions and manipulations were carried out under an inert atmosphere of purified nitrogen using standard Schlenk-tube techniques. Solvents were dried and distilled under nitrogen before use: hexane and toluene over sodium, tetrahydrofuran and diethyl ether over sodium−benzophenone, dichloromethane over phosphorus pentoxide. Nitrogen (Air liquide, R-grade) was passed through BASF R3-11 catalyst and molecular sieve columns to remove residual oxygen and water. Elemental C, H, and N analyses were performed by the Service de microanalyses du CNRS (ULP Strasbourg). Infrared spectra were recorded on a IFS 66 Bruker FT-IR spectrometer. The ^{1}H and ^{31}P{^{1}H} spectra were recorded at 300.1 and 121.5 MHz, respectively, on a Bruker AM300 instrument and the ^{119}Sn NMR spectra at 149 MHz on a Bruker AC400 instrument. Fe(CO)$_5$ was obtained from Aldrich, and HSiMe(OSiMe$_3$)$_2$ was provided by Rhône-Poulenc Spécialités Chimiques; both were used as received. The complexes [Pd(η^3-allyl)(μ-Cl)]$_2$,[39] **1a**,[31] **2a**,[32] **3a**,[33] and **3b**[32] were prepared according to published procedures. Ph$_3$SnH was obtained by reduction of Ph$_3$SnCl with LiAlH$_4$ in diethyl ether.[40] ^{n}Bu$_3$SnH was a commercial sample (Lancaster) and was used as received. Experimental errors on the TON and TOF values have been estimated to 5%; values given have been rounded off.

Synthesis of [(OC)$_3$Fe{SiMe(OSiMe$_3$)$_2$}(μ-Ph$_2$Ppy)Pd(η^3-allyl)] (2b). A magnetically stirred solution of [Fe(CO)$_5$] (1.57 mL, 12 mmol) and HSiMe(OSiMe$_3$)$_2$ (5.00 g, 22.5 mmol) in hexane (100 mL) was irradiated in a 2-propanol-cooled photochemical reactor at 283 K for ca. 4 h. Irradiation with a mercury lamp (180 W, TQ 150, Hereaus) was stopped when the ν(CO) absorptions of [Fe(CO)$_5$] (2001 and 2023 cm^{-1}) had almost completely disappeared. The resulting complex, *cis*-[HFe{SiMe(OSiMe$_3$)$_2$}(CO)$_4$] (ν(CO) (hexane) 2096 m, 2032 sh, 2026 vs, 2013 vs cm^{-1}), was not isolated, and the resulting pale yellow mixture was added immediately to a toluene solution (50 mL) of (2-diphenylphosphino)pyridine (2.89 g, 11 mmol) in two portions. After each addition the CO evolved was removed under reduced pressure for 1 min. The solution was stirred for 5 min at room temperature and then placed at −20 °C for 2−3 days, which afforded *mer*-[HFe(CO)$_3${SiMe(OSiMe$_3$)$_2$}(Ph$_2$Ppy-*P*)] (**4**) as a pale brown air- and moisture-sensitive solid (4.40 g, yield 64%), which was rapidly engaged in further reactions. IR (toluene): 2051 w, 1987 s, 1975 vs cm^{-1}. ^{1}H NMR (C$_6$D$_6$, 298 K): δ −8.87 (d, ^2J(P−H) = 26 Hz, 1H, Fe−H), 0.31 (s, 18H, OSi*Me*$_3$), 0.93 (s, 3H, Fe−SiMe), 6.3−8.5 (m, 14H, aromatics). ^{31}P{^{1}H} NMR (C$_6$D$_6$, 298 K): 63.2.

Solid complex **4** (1.50 g, 2.4 mmol) was added to a suspension of excess KH in THF (20 mL). An immediate gas evolution was noticed (H$_2$), whereupon the color darkened. The formation of K[Fe{SiMe(OSiMe$_3$)$_2$}(CO)$_3$(Ph$_2$Ppy-*P*)] (**5**) was complete after ca. 30 min. The solution was then filtered over a 1 cm Celite pad and slowly added to a THF solution (10 mL) of [Pd(η^3-allyl)(μ-Cl)]$_2$ (0.44 g, 1.2 mmol) at 233 K. The reaction mixture was warmed to room temperature and stirred for 1 h before it was filtered. The volatiles were removed under reduced pressure, and the residue was dissolved in diethyl ether and filtered over a 5 cm Celite pad placed in a pipet. The solvent was then removed in vacuo, affording complex **2b** as a yellow-orange air-stable powder (1.33 g, yield 72%). IR (KBr): 1955 m, 1895 s, 1873 vs cm^{-1}. ^{1}H NMR (C$_6$D$_6$, 298 K; for the labeling of the allyl protons, see below): δ 0.49 (s, 18H, OSiMe$_3$), 2.82 (d, 1H, ^3J(H−H) = 11.25 Hz, allyl H^3), 3.11 (d, 1H, ^3J(H−H) = 12.85 Hz, allyl H^2), 3.66 (d, 1H, ^3J(H−H) = 6.26 Hz, allyl H^4), 4.29 (br, 1H, allyl H^1), 5.04 (m, 1H, allyl H^5), 6.12−8.30 (m, 14H, aromatics). ^{31}P{^{1}H} NMR (C$_6$D$_6$, 298 K): 73.3. Anal. Calcd for C$_{30}$H$_{40}$FeNO$_5$PPdSi$_3$: C, 46.67; H, 5.22; N, 1.81. Found: C, 46.94; H, 5.25; N, 1.86.

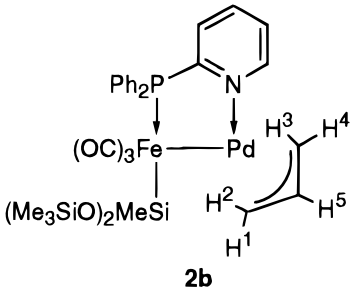

2b

Dehydrogenative Coupling of Ph$_3$SnH Catalyzed by 1a, 2a,b, and 3a,b. General Procedure. A Schlenk flask equipped with a stirring bar and a serum cap was charged with 4.00 g of Ph$_3$SnH (11.4 mmol) in 15 mL of CH$_2$Cl$_2$ and was placed in a water bath at 293 K.

H$_2$ Monitoring (2a,b and 3b). When the volume of H$_2$ released was monitored, the procedure was as follows: the Schlenk flask was fitted onto a gas buret and 1.0 mL of a 0.1 mM solution of catalyst (10^{-4} mmol) was rapidly added to the reaction mixture via syringe through the serum cap. The volume of H$_2$ released was directly read on the graduated buret, taking into account the content of the syringe. The turnover numbers were calculated by the following equation: TON = moles of H$_2$/mol of catalyst, with moles of H$_2$ being determined by applying the gas equation: $PV = nRT$. Each experiment was repeated at least three times, and the mean values were used for the plots. When the reaction was over, the volatiles were removed in vacuo and the residue was washed with Et$_2$O, affording Ph$_6$Sn$_2$ as a white solid (mp 225−235 °C;[41,42] the ^{1}H NMR spectrum only showed signals in the aromatic region). The TON determined from the amount of Ph$_6$Sn$_2$ recovered was in all cases in good accordance with that determined from the volumes of H$_2$.

Ph$_6$Sn$_2$ Monitoring (1a and 3a). When the formation of Ph$_6$Sn$_2$ was monitored, the procedure was as follows: a battery of five Schlenk tubes was prepared as described above, except that they were not connected to gas burets. The catalyst was then added, and the reaction mixtures were successively quenched at t = 1, 4, 8, 24, and 72 h by addition of water. The volatiles were removed under reduced pressure, and the residue was washed with Et$_2$O, affording pure Ph$_6$Sn$_2$ as a white solid, which was weighed. The turnover numbers were determined by the following equation: TON = (moles of Ph$_6$Sn$_2$)/(moles of catalyst). The purity of Ph$_6$Sn$_2$ was controlled by ^{119}Sn NMR spectroscopy (149 MHz, CH$_2$Cl$_2$/C$_6$D$_6$): δ −143.7 ppm with satellites, similar to the literature value of −144 ppm (CDCl$_3$).[43] A catalytic reaction was carried out in only 5 mL of CH$_2$Cl$_2$ in order to obtain a concentrated supernatant solution, which was examined by ^{119}Sn NMR spectroscopy before quenching. It contained more than 88% Ph$_6$Sn$_2$ and small amounts of Ph$_3$SnCl (δ −44.7 ppm) and Ph$_3$SnH (δ −165

(38) (a) Braunstein, P.; Rosé, J. In *Comprehensive Organometallic Chemistry II*; Abel, E. W., Stone, F. G. A., Wilkinson, G., Eds.; Pergamon: Oxford, U.K., 1995; Vol. 10, pp 351−385. (b) Braunstein, P.; Rosé, J. In *Metal Clusters in Chemistry*; Braunstein, P., Oro, L. A., Raithby, P. R., Eds.; Wiley-VCH: Weinheim, Germany, 1999; Vol. 2, pp 616−677. (c) Braunstein, P.; Knorr, M.; Stern, C. *Coord. Chem. Rev.* **1998**, *178−180*, 903.

(39) Sakakibara, M.; Takahashi, Y.; Sakai, S.; Ishii, Y. *J. Chem. Soc., Chem. Commun.* **1969**, 396.

(40) Kuivila, H. G.; Sawyer, A. K.; Armour, A. G. *J. Org. Chem.* **1961**, *26*, 1426.

(41) Tamborski, C.; Ford, F. E.; Soloski, E. J. *J. Org. Chem.* **1963**, *28*, 237.

(42) Gilman, H.; Rosenberg, S. D. *J. Org. Chem.* **1953**, *18*, 1554.

(43) Adams, S.; Dräger, M.; Mathiasch, B. *J. Organomet. Chem.* **1987**, *326*, 173.

Table 4. Crystallographic Data for Complex 2b

mol formula	$C_{30}H_{41}FeNO_5PdSi_3$
mol wt	773.14
cryst syst	orthorhombic
space group	$Pna2_1$
a, Å	17.888(2)
b, Å	23.967(4)
c, Å	8.652(2)
V, Å^3	3709(1)
Z	4
D_{calcd}, g cm^{-3}	1.384
$F(000)$	1588
μ(Cu Kα), cm^{-1}	10.51
no. of measd rflns	6616
no. of obsd data measd ($I \geq 2\sigma(I)$)	1807
no. of unique data obsd	1024
no. of variables	200
GOF[a]	1.008
$R(F_o)$[b]	0.037
$R_w(F_o)$[c]	0.039

[a] GOF $= [\sum w(|F_o| - |F_c|)^2/(N_{observns} - N_{variables})]^{1/2}$. [b] $R = \sum||F_o| - |F_c||/\sum|F_o|$. [c] $R_w = [\sum w(|F_o| - |F_c|)^2/\sum w(F_o)^2]^{1/2}$.

ppm); no resonance for $(Ph_3Sn)_2O$ (δ −82.7 ppm), which could have formed by adventitious oxidation, was observed.

Dehydrogenative Coupling of ^{n}Bu$_3$SnH. A procedure similar to that described above for the H_2 monitoring in dehydrogenative coupling of Ph_3SnH was used, with typically 5.00 g of ^{n}Bu$_3$SnH (17.2 mmol) and 0.5 mL of a 3.45×10^{-5} M solution of the catalyst ((moles of ^{n}Bu$_3$SnH)/(moles of catalyst) = ca. 1 000 000), except in the case of catalyst **3a**, which was used as a 6.9×10^{-6} M solution. A vigorous H_2 evolution was immediately observed in all cases. Analysis of the catalytic mixture by ^{119}Sn NMR spectroscopy showed the very intense signal of ^{n}Bu$_6$Sn$_2$ at δ −83 ppm and a very weak signal (<2%) at δ 83 ppm, which corresponds to the value for $(^n$Bu$_3$Sn$)_2$O.

X-ray Structure Determination of 2b. X-ray data were collected on a Philips PW 1100 diffractometer using graphite-monochromated Mo Kα radiation (λ = 0.710 73 Å). Crystal data and experimental details are summarized in Table 4. The intensities were corrected for Lorentz and polarization. An empirical absorption correction was applied (maximum and minimum transmission factors 1.00−0.598).[44] The structure was solved by direct methods using SIR92[45] and refined by blocked full-matrix least squares based on F using SHELX76.[46] Only the Pd, Fe, P, and Si atoms were refined anisotropically. All the hydrogen atoms, except those of the allyl group, were placed at their at their geometrically calculated positions and refined "riding" on their corresponding carbon atoms. All the calculations were carried out on the GOULD ENCORE91 computer of the Centro di Studio per la Strutturistica Diffrattometrica of the CNR, Parma, Italy.

Atomic coordinates of the non-hydrogen atoms (Table S1; Supporting Information), thermal parameters for the non-hydrogen atoms (Table S2), atomic coordinates of the hydrogen atoms (Table S3), and all bond distances and angles (Table S4) have been deposited at the Cambridge Crystallographic Data Centre.

Acknowledgment. Financial support from the Centre National de la Recherche Scientifique (Paris), the Consiglio Nazionale delle Ricerche (Roma), and the Ministère de l'Education Nationale, de la Recherche et de la Technologie (Paris) (Ph.D. grant to J.D.) are gratefully acknowledged. We also thank Rhône-Poulenc Spécialités Chimiques for a gift of $HSiMe(OSiMe_3)_2$.

Supporting Information Available: Tables of X-ray crystallographic data for **2b**. This material is available free of charge via the Internet at http://pubs.acs.org.

OM9906619

(44) Walker, N.; Stuart, D. *Acta Crystallogr., Sect. A* **1983**, *39*, 158. Ugozzoli, F. *Comput. Chem.* **1987**, *11*, 109.

(45) Altomare, A.; Burla, M. C.; Camalli, M.; Cascarano, G.; Giacovazzo, C.; Guagliardi, A.; Polidori, G. SIR92. *J. Appl. Crystallogr.* **1994**, *27*, 435.

(46) Sheldrick, G. SHELX76, Program for Crystal Structure Determinations; University of Cambridge, Cambridge, U.K., 1976.